Jovasevic et al., http://www.jcb.org/cgi/content/full/jcb.201505123/DC1.

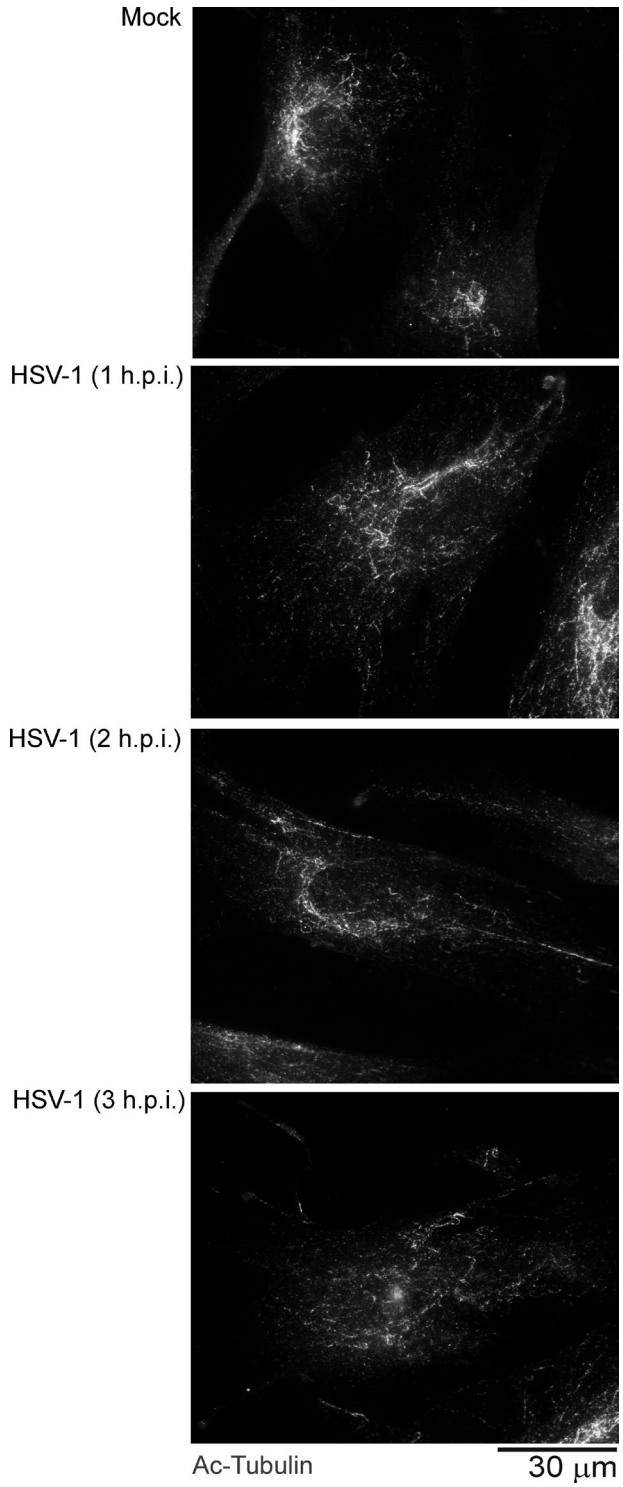

Figure S1. **Ac-tubulin staining in HSV-1–infected NHDFs.** Single-channel grayscale images of Ac-tubulin staining from panels shown in Fig. 1 B are provided, illustrating the lack of Ac-MT induction in the early stages of HSV-1 infection. NHDFs were mock infected or infected with HSV-1 at MOI 20 for the indicated times in hpi.

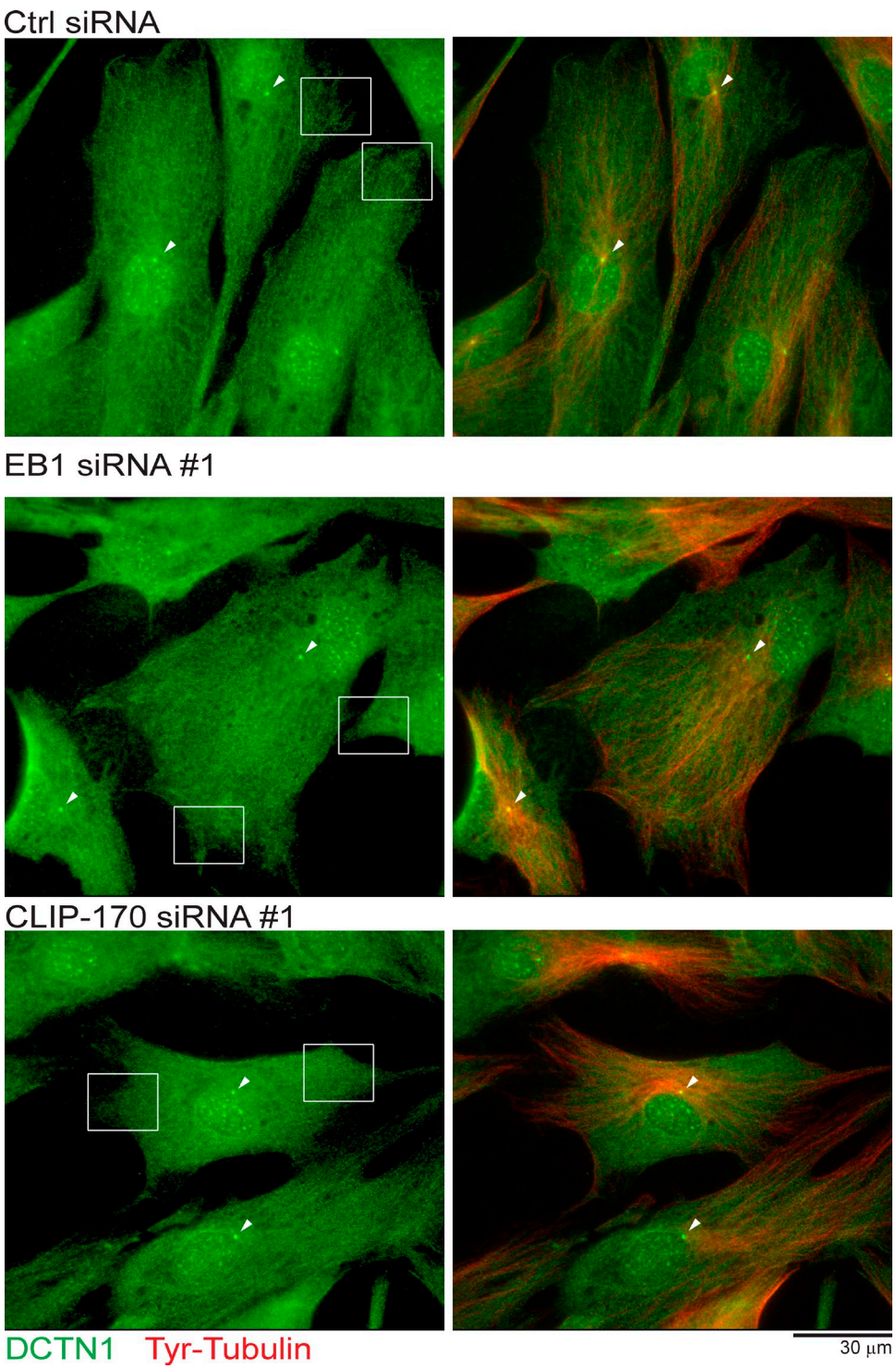

Figure S2. **Effects of CLIP-170 or EB1 depletion on the distribution of DCTN1 in primary NHDFs.** NHDFs were treated with control, nontargeting siRNA, or siRNAs targeting EB1 or CLIP-170. Cultures were fixed and stained for Tyr-tubulin (red) or DCTN1 (green). Images were acquired using a DMI6000B microscope, and representative fields are shown. Arrowheads point to concentrations of DCTN1 and Tyr-tubulin at centrosomes. Boxes highlight examples of flecked patterns of DCTN1 staining at the cell periphery evident in control samples, which appear more diffuse in NHDFs depleted of either EB1 or CLIP-170.

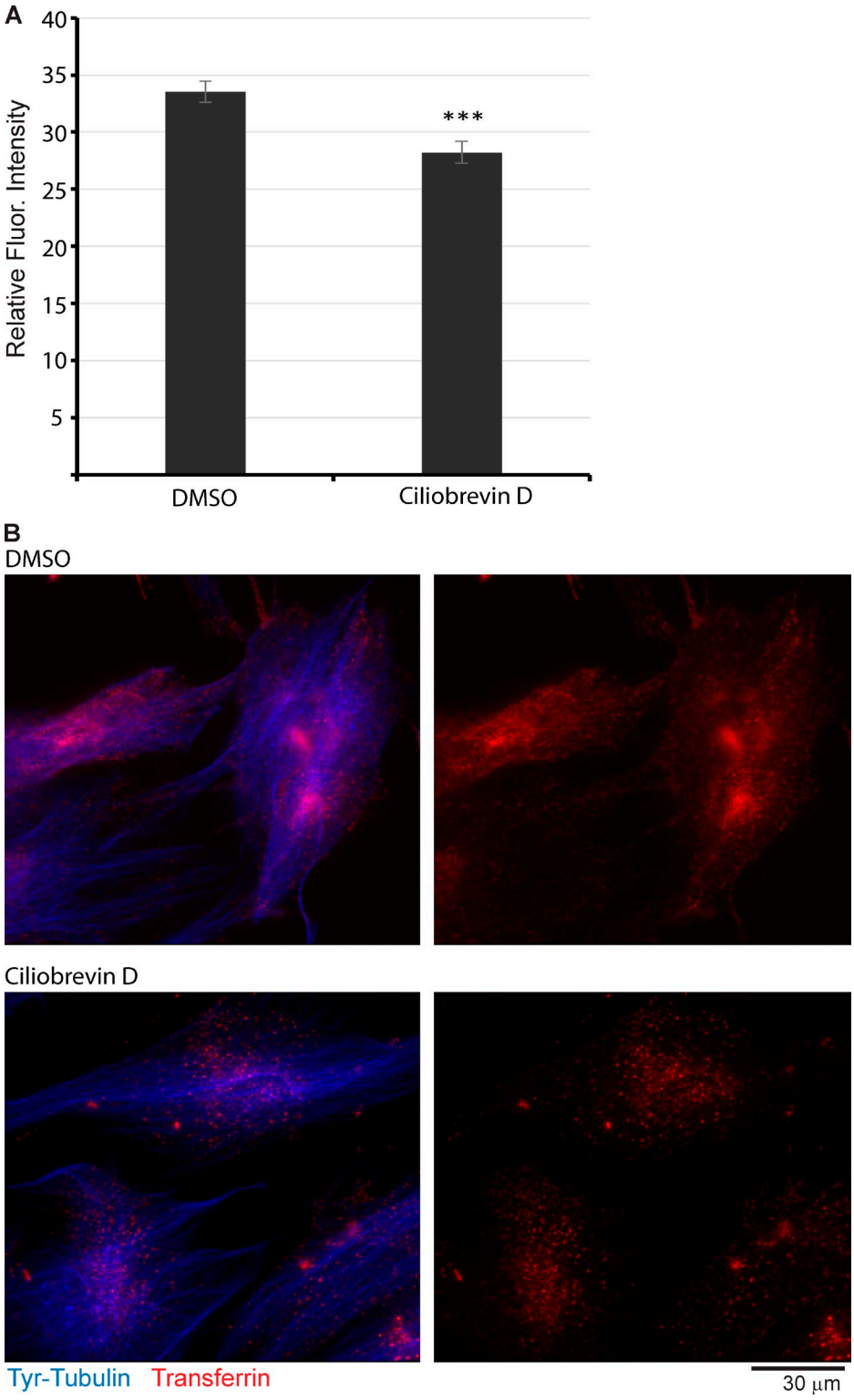

Figure S3. **Transferrin uptake and distribution in ciliobrevin D–treated NHDFs.** NHDFs were treated with DMSO solvent control or 200-μM ciliobrevin D for 1 h. Cultures were then incubated for 30 min with fluorescently labeled transferrin (red). (A) Transferrin uptake was determined by quantifying the fluorescence intensity of transferrin signal (arbitrary units) in samples. Error bars represent standard error of the mean. ***, $P < 0.0001$ versus DMSO group (one-way ANOVA; $n = 20$/group; $F_{(1,38)} = 15.629$; $P < 0.0001$). (B) Samples were stained for Tyr-tubulin (blue) and imaged using a DMI6000B-AFC microscope and a 100× objective. Representative widefield images are shown.

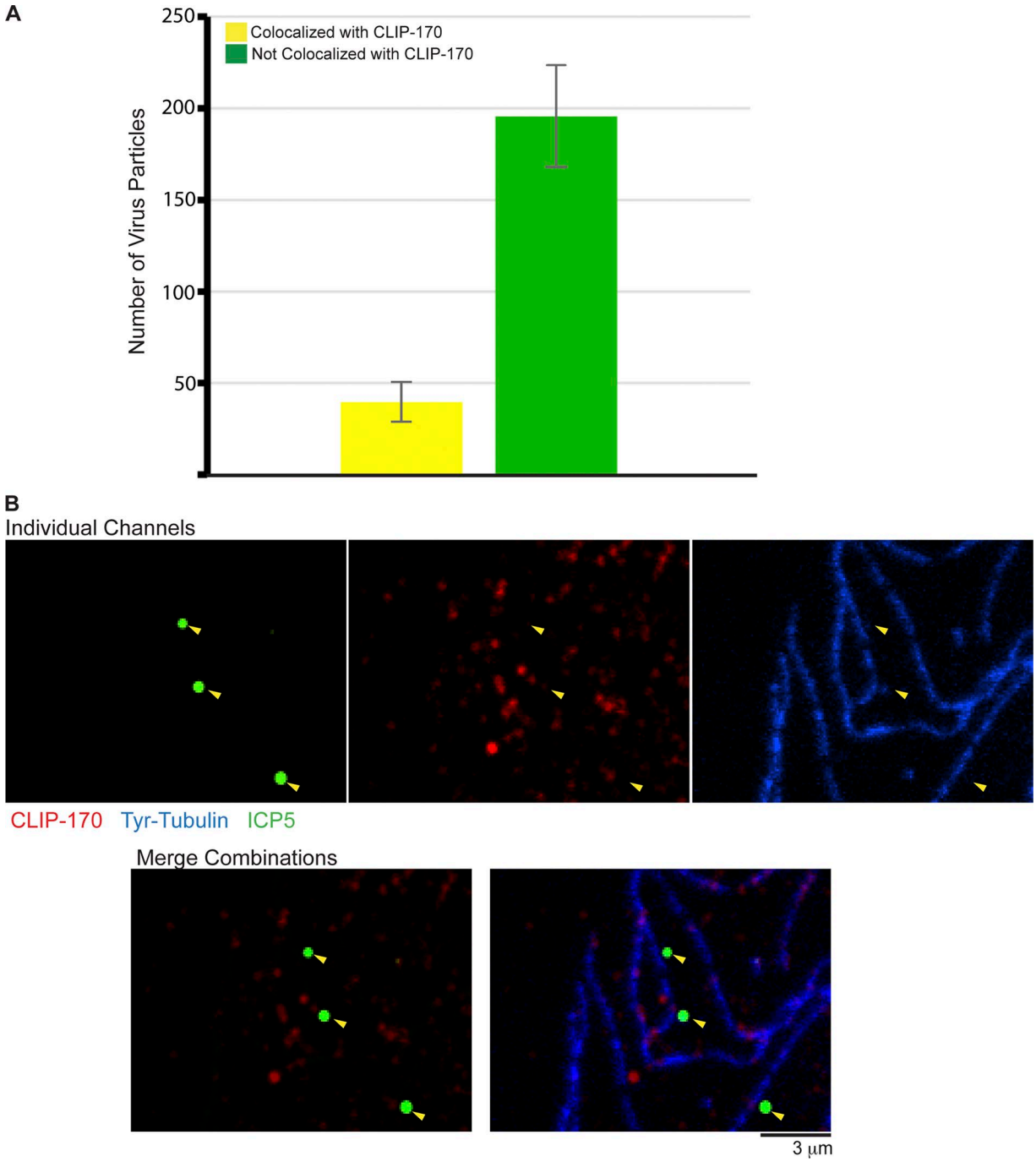

Figure S4. **Colocalization of HSV-1 with CLIP-170 and its requirement for EB1.** (A) Quantification of capsids colocalized (yellow) or not colocalized (green) with CLIP-170 determined ~16% colocalization in random fields of view from samples described in Fig. 6 A. *n* = 166–281 particles per field. Error bars represent standard error of the mean between three experiments. (B) NHDFs were treated with EB1 siRNA and then infected with HSV-1 at MOI 20 for 4 h. Fixed samples were stained for ICP5 (green), CLIP-170 (red), and Tyr-tubulin (blue). A representative confocal image is shown. Yellow arrowheads point to examples of HSV-1 capsids that fail to colocalize with CLIP-170 patches found along the MT lattice.

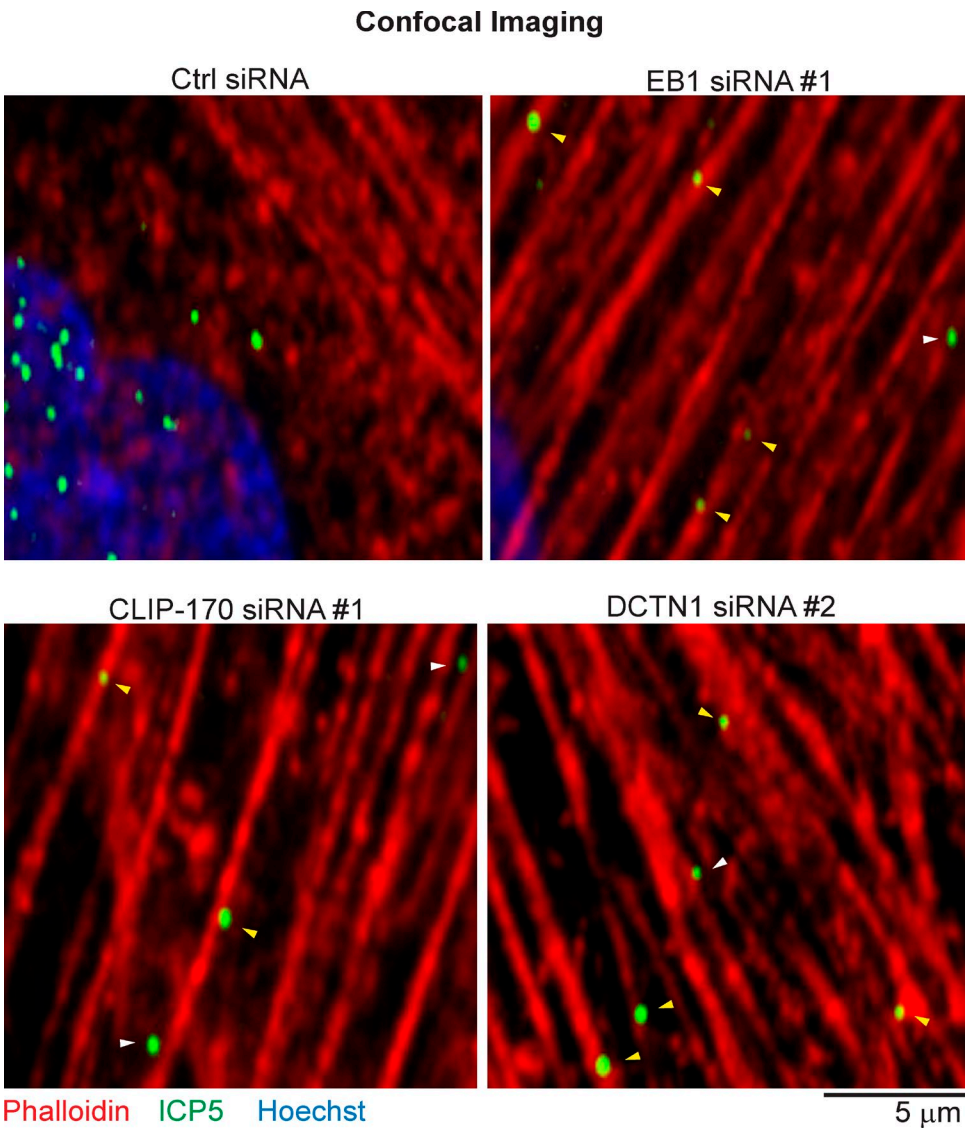

Figure S5. **HSV-1 capsids localize to actin filaments in cells depleted of EB1, CLIP-170, or DCTN1.** NHDFs were treated with control, EB1, CLIP-170, or DCTN1 siRNAs and then infected with HSV-1 at MOI 20 for 3 h. Fixed samples were stained with phalloidin-647 (red) and anti-ICP5 monocolonal antibody (green). Nuclei were stained with Hoechst (blue). Representative confocal images are shown illustrating capsid localization to actin filaments (highlighted by arrowheads) in NHDFs depleted of EB1, CLIP-170, or DCTN1.

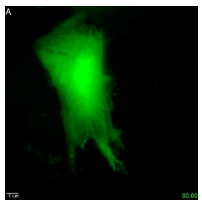

Video 1. **Time-lapse of EB1-DN in NHDFs, and HSV-1 motility in ciliobrevin D–treated NHDFs.** (A) NHDFs were transfected with pN1-EB1-mCherry (false-colored green for contrast) encoding dominant-negative EB1 (EB1-DN) using Lipofectamine 3000. 24 h after transfection, cells were analyzed using time-lapse microscopy on a DMI6000B-AFC widefield microscope with a 100× objective. Images were acquired at 4 fps for 37 s. The playback speed of the video is 15 fps (i.e., ~4× real speed). A representative cell is shown. (B) NHDFs were treated with 200-μM ciliobrevin D for 1 h and then infected with HSV-1 containing a GFP-tagged capsid protein, VP26 (K26GFP; green). 3 hpi, nuclei were stained with Hoechst (blue) and cells were analyzed using time-lapse microscopy on a DMI6000B-AFC widefield microscope with a 100× objective using an environmental chamber at 37°C. Images were captured at 1 fps for 155 s. The playback speed of the video is 15 fps (i.e., ~15× real speed). A representative video illustrates the brief but abortive long-range motility of virus particles in the presence of dynein inhibitor.

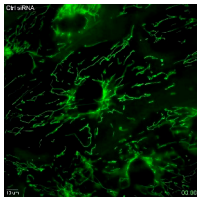

Video 2. **Movement of mitochondria in control or EB1 siRNA–treated NHDFs.** NHDFs were treated with control siRNA (left) or EB1 siRNA #1 (right) and then treated with MitoTracker (green) as described in Materials and methods section Antibodies, WB, IF, and imaging. Cells were analyzed using time-lapse microscopy on a DMI6000B-AFC widefield microscope with a 100× objective using an environmental chamber at 37°C. Images were captured at 0.3 fps for 3 min. The playback speed of the video is 15 fps (i.e., ∼50× real speed).

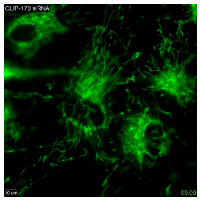

Video 3. **Movement of mitochondria in NHDFs depleted of CLIP-170 or DCTN1.** NHDFs were treated with CLIP-170 siRNA #1 (left) or DCTN1 siRNA #2 (right) and then treated with MitoTracker (green) as described in Materials and methods section Antibodies, WB, IF, and imaging. Cells were analyzed using time-lapse microscopy on a DMI6000B-AFC widefield microscope with a 100× objective using an environmental chamber at 37°C. Images were captured at 0.3 fps for 3 min. The playback speed of the video is 15 fps (i.e., ∼50× real speed).

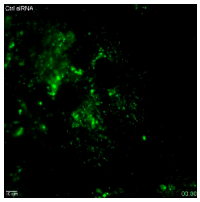

Video 4. **Movement of lysosomes in control or EB1 siRNA–treated NHDFs.** NHDFs were treated with control siRNA (left) or EB1 siRNA #1 (right) and then treated with LysoTracker (green) as described in Materials and methods section Antibodies, WB, IF, and imaging. Cells were analyzed using time-lapse microscopy on a DMI6000B-AFC widefield microscope with a 100× objective using an environmental chamber at 37°C. Images were captured at 2 fps for 48 s. The playback speed of the video is 30 fps (i.e., ∼15× real speed).

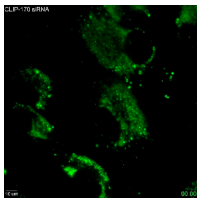

Video 5. **Movement of lysosomes in NHDFs depleted of CLIP-170 or DCTN1.** NHDFs were treated with CLIP-170 siRNA #1 (left) or DCTN1 siRNA #2 (right) and then treated with LysoTracker (green) as described in Materials and methods section Antibodies, WB, IF, and imaging. Cells were analyzed using time-lapse microscopy on a DMI6000B-AFC widefield microscope with a 100× objective using an environmental chamber at 37°C. Images were captured at 2 fps for 30–50 s. The playback speed of the video is 30 fps (i.e., ∼15× real speed).

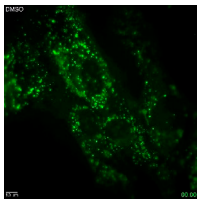

Video 6. **Movement of lysosomes in DMSO- or ciliobrevin D–treated NHDFs.** NHDFs were treated with DMSO solvent control (left) or 200-µM ciliobrevin D (CbD; right) for 1 h and then stained with LysoTracker (green) as described in Materials and methods section Antibodies, WB, IF, and imaging. Cells were analyzed using time-lapse microscopy on a DMI6000B-AFC widefield microscope with a 100× objective using an environmental chamber at 37°C. Images were captured at 2 fps for 50 s. The playback speed of the video is 30 fps (i.e., ∼15× real speed).

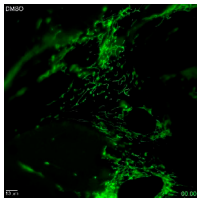

Video 7. **Movement of mitochondria in DMSO- or ciliobrevin D–treated NHDFs.** NHDFs were treated with DMSO solvent control (left) or 200-µM ciliobrevin D (CbD; right) for 1 h and then stained with MitoTracker (green) as described in Materials and methods section Antibodies, WB, IF, and imaging. Cells were analyzed using time-lapse microscopy on a DMI6000B-AFC widefield microscope with a 100× objective using an environmental chamber at 37°C. Images were captured at 0.3 fps for 3 min. The playback speed of the video is 15 fps (i.e., ∼50× real speed).

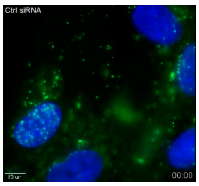

Video 8. **HSV-1 capsid movement in control siRNA–treated NHDFs.** NHDFs were treated with control, nontargeting siRNAs and then infected with HSV-1 containing a GFP-tagged capsid protein, VP26 (HSV-1 K26GFP; green). 3 hpi, nuclei were stained with Hoechst (blue). Cells were analyzed using time-lapse microscopy on a DMI6000B-AFC widefield microscope with a 100× objective using an environmental chamber at 37°C. Images were captured at 1 fps for ~400 s. The playback speed of the video is 15 fps (i.e., ~15× real speed). Virus particles at different stages of transport and infection could be observed. Two representative videos are shown that illustrate these different stages (left and right). Many particles had reached and brightly lit the nucleus, while those remaining in the cytoplasm exhibited rapid, long-range movements characteristic of MT-based motility. Particles were also observed moving in and out of, and even forming, perinuclear clusters that represent the centrosome, while others could be seen approaching the nucleus.

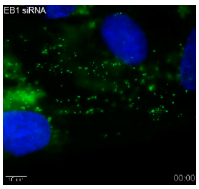

Video 9. **HSV-1 capsid movement in EB1- or CLIP-170–depleted NHDFs.** NHDFs were treated with EB1 siRNA #1 (left) or CLIP-170 siRNA #1 (right) and then infected with HSV-1 K26GFP (green). 3 hpi, nuclei were stained with Hoechst (blue). Cells were analyzed using time-lapse microscopy on a DMI6000B-AFC widefield microscope with a 100× objective using an InVivo environmental chamber at 37°C. Images were captured at 1 fps for ~400 s. The playback speed of the video is 15 fps (i.e., ~15× real speed). In EB1- or CLIP-170–depleted cells, viral particles remain at the cell periphery and fail to initiate long-range transport to the nucleus.

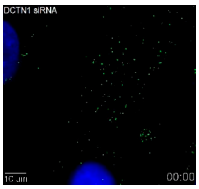

Video 10. **HSV-1 capsid movement in NHDFs transfected with DCTN1-siRNA or expressing EB1-DN.** NHDFs transfected with DCTN1 siRNA #2 (left) or expressing dominant-negative EB1 (EB1-DN; right) were infected with HSV-1 K26GFP (green). 3 hpi, nuclei were stained with Hoechst (blue). Cells were analyzed using time-lapse microscopy on a Leica DMI6000B-AFC widefield microscope with a 100× objective using an InVivo environmental chamber at 37°C. Images were captured at 1 fps for ~330 s. The playback speed of the video is 15 fps (i.e., ~15× real speed). In DCTN1-depleted cells or cells expressing dominant-negative EB1, viral particles remain at the cell periphery and fail to initiate long-range transport to the nucleus.